European Journal of Inorganic Chemistry

Supporting Information

Unique Dimerization Topology and Countercation Binding Modes in 12-Metallacrown-4 Compounds

Elvin V. Salerno, Collin M. Foley, Vittoria Marzaroli, Bernadette L. Schneider, Max D. Sharin, Jeff W. Kampf, Luciano Marchiò, Matthias Zeller, Régis Guillot, Talal Mallah,* Matteo Tegoni,* Vincent L. Pecoraro,* and Curtis M. Zaleski*

Table of Contents

Additional Refinement Details for 1-7

For **1** minor whole molecule disorder was detected for the metallacrown molecule and all organic fragments (excluding the dysprosium and sodium ions), and the occupancy ratio refined to 0.8948(8) to 0.1052(8).[1] In addition, DMF and water molecules, both coordinated to metal ions and interstitial, were highly disordered with most DMF molecules refined as disordered over two alternative orientations, and some over three orientations and/or to be disordered with water molecules.[1] For **2** the whole main molecule exhibits disorder by a pseudo-mirror operation (excluding the dysprosium and sodium ions) and the occupancy ratio refined to 0.8498(15) to 0.1502(15). An interstitial DMF molecule was refined as independently disordered and the occupancy ratio refined to 0.462(6) to 0.538(6). For **4** whole molecule disorder was detected for the metallacrown molecule and all organic fragments (excluding the ytterbium and sodium ions), and the occupancy ratio refined to 0.719(2) to 0.281(2). An interstitial DMF molecule was refined as independently disordered, and the occupancy ratio refined to 0.566(14) to 0.434(14). For **6** whole molecule disorder was detected for the metallacrown molecule and all organic fragments (excluding the yttrium ion), and the occupancy ratio was set to 0.8 to 0.2. An interstitial DMF molecule was disordered over two orientations each with 0.5 occupancy. For **7** whole molecule disorder was detected for the metallacrown molecule and all organic fragments (excluding the holmium ions), and the occupancy ratio refined to 0.7831(11) to 0.2169(11). For **1**-**7** the U_{iso} values for hydrogen atoms were set to a multiple of the value of the carrying carbon atom (1.2 times for sp^2 hybridized carbon atoms or 1.5 times for methyl carbon atoms).

Table S1. Crystallographic parameters for **1 - 7**.

Compound	**1**[1]	**2**	**3**	**4**	**5**	**6**	**7**
CCDC No.	2030729	2163142	2163140	2163143	2163145	2163141	2163144
Chemical formula	$C_{146.38}H_{191.01}Dy_2Mn_8N_{27.46}Na_2O_{63.41}$	$C_{116}H_{120}Dy_2Mn_8N_{16}Na_{24}O_{64}$	$C_{84}H_{64}Dy_2Mn_8N_{12}Na_2O_{50}$	$C_{116}H_{128}Ga_8N_{16}Na_2O_{80}Yb_2$	$C_{158}H_{130}Dy_2Ga_8N_{16}O_{46}S_8$	$C_{131}H_{105.40}Ga_8N_{22.60}O_{43.404}Y_2$	$C_{130.15}H_{144.01}Ga_9Ho_2N_{26.22}O_{55.08}$
Formula weight (g/mol)	4160.38	3572.77	2851.97	3976.16	4128.01	3426.15	3914.29
Crystal system	Triclinic	Tetragonal	Tetragonal	Tetragonal	Monoclinic	Monoclinic	Monoclinic
Temperature (K)	150(2)	150(2)	85(2)	100(1)	85(2)	100	215
λ (Å)	0.71073	0.71073	1.54184	1.54178	1.54184	0.700	0.71073
Space group	$P\bar{1}$	I4/m	I4/m	I4/m	$P2_1/c$	$P2_1/c$	$P2_1$
a (Å)	17.4390(17)	17.7273(6)	17.91240(10)	17.6035(5)	24.6387(4)	13.9719(2)	14.1210(10)
b (Å)	17.4009(19)	17.7273(6)	17.91240(10)	17.6035(5)	29.1380(6)	38.5773(6)	38.892(3)
c (Å)	19.446(2)	31.7170(13)	31.1113(3)	31.3671(9)	23.4319(4)	14.0473(3)	17.3588(13)
α (°)	64.372(5)	90	90	90	90	90	90
β (°)	64.955(5)	90	90	90	90.094(2)	90.620(2)	103.7400(10)
γ (°)	66.057(5)	90	90	90	90	90	90
Volume ($Å^3$)	4637.5(9)	9967.3(8)	9982.19(15)	9720.1(6)	16822.3(5)	7571.0(2)	9260.7(12)
Z	1	2	2	2	4	2	2
Density (calculated), Mg/m^3	1.490	1.190	0.949	1.359	1.630	1.503	1.404
μ (mm^{-1})	1.414	1.304	8.402	3.691	7.697	2.145	2.209
F(000)	2122.8	3588	2812	3972	8264	3446	3924
Limiting indices	$-24 \le h \le 24$, $-24 \le k \le 24$, $-27 \le \ell \le 27$	$-23 \le h \le 23$, $-20 \le k \le 23$, $-42 \le \ell \le 42$	$-21 \le h \le 21$, $-21 \le k \le 21$, $-37 \le \ell \le 37$	$-21 \le h \le 21$, $-21 \le k \le 21$, $-37 \le \ell \le 37$	$-28 \le h \le 28$, $-34 \le k \le 31$, $-27 \le \ell \le 27$	$-17 \le h \le 17$, $-48 \le k \le 48$, $-17 \le \ell \le 17$	$-18 \le h \le 18$, $-49 \le k \le 49$, $-22 \le \ell \le 22$
Goodness-of-fit	1.029	1.122	1.068	1.080	1.118	1.079	1.021
R_1	0.0554 [I>2σ(I)]; 0.0829 (all data)	0.0360 [I>2σ(I)]; 0.0403 (all data)	0.0517 [I>2σ(I)]; 0.0532 (all data)	0.0603 [I>2σ(I)]; 0.0613 (all data)	0.0937 [I>2σ(I)]; 0.1562 (all data)	0.0716 [I>2σ(I)]; 0.0736 (all data)	0.0622 [I>2σ(I)]; 0.0764 (all data)
wR_2	0.1213 [I>2σ(I)]; 0.1355 (all data)	0.1002 [I>2σ(I)]; 0.1048 (all data)	0.1553 [I>2σ(I)]; 0.1572 (all data)	0.1656 [I>2σ(I)]; 0.1665 (all data)	0.2105 [I>2σ(I)]; 0.2526 (all data)	0.2103 [I>2σ(I)]; 0.2117 (all data)	0.1549 [I>2σ(I)]; 0.1629 (all data)

Table S2. Average bond length and bond valence sum values used to support the assigned metal oxidation states of **1-7**.

	Avg. Bond Length (Å)	Bond valence sum value (v.u.)	Assigned Oxidation State
1, **$Dy_2Mn_8Na_2(iph)_4$**[1]			
Dy	2.367	3.08	3+
Mn1	2.048	3.13	3+
Mn2	2.038	3.12	3+
Mn3	2.047	3.08	3+
Mn4	2.042	3.13	3+
2, **$Dy_2Mn_8Na_2(tma)_4$**			
Dy	2.366	3.07	3+
Mn	2.039	3.10	3+
3, **$Dy_2Mn_8Na_2(dnic)_4$**			
Dy	2.350	3.16	3+
Mn	2.025	3.14	3+
4, **$Yb_2Ga_8Na_2(tma)_4$**			
Yb	2.303	3.12	3+
Ga	1.985	3.42	3+
5, **$Dy_2Ga_8(Hpy)_2(dtba)_4$**			
Dy1	2.363	3.06	3+
Dy2	2.366	3.03	3+
Ga1	1.918	3.21	3+
Ga2	1.995	3.32	3+
Ga3	1.909	3.29	3+
Ga4	1.995	3.29	3+
Ga5	1.908	3.29	3+
Ga6	1.994	3.30	3+
Ga7	1.903	3.34	3+
Ga8	1.983	3.43	3+
6, **$Y_2Ga_8(Hpy)_2(dnic)_4$**			
Y	2.321	3.50	3+
Ga1	2.005	3.24	3+
Ga2	1.999	3.29	3+
Ga3	1.913	3.24	3+
Ga4	1.994	3.30	3+
7, **$Ho_2Ga_8(Ga\text{-}OH)(dnic)_4$**			
Ho1	2.326	3.25	3+
Ho2	2.334	3.19	3+
Ga1	1.919	3.21	3+
Ga2	1.992	3.35	3+
Ga3	1.993	3.16	3+
Ga4	2.006	3.13	3+
Ga5	1.998	3.27	3+
Ga6	1.916	3.22	3+
Ga7	1.979	3.32	3+
Ga8	1.971	3.38	3+
Ga1L	2.140	2.11	3+

Table S3. Continuous Shape Measurement (CShM) values (*SHAPE 2.1*) for the eight-coordinate central Ln^{III} ions of **1 - 7**.

Shape	**1**[1]	**2**	**3**	**4**	**5**		**6**	**7**	
	Dy	Dy	Dy	Yb	Dy1	Dy2	Y	Ho1	Ho2
Octagon (D_{8h})	33.099	32.354	31.097	31.067	29.497	29.687	32.177	31.114	31.009
Heptagonal Pyramid (C_{7v})	23.468	23.598	23.665	23.664	23.540	23.497	23.232	23.160	22.678
Hexagonal Bipyramid (D_{6h})	16.261	16.528	16.919	16.246	17.598	17.543	16.115	15.949	16.089
Cube (O_h)	8.700	8.880	9.305	8.571	10.563	10.464	8.967	8.880	8.867
Square Antiprism (D_{4d})	**0.885**	**0.708**	**0.430**	**0.518**	**0.662**	**0.689**	**0.624**	**0.518**	**0.518**
Triangular Dodecahedron (D_{2d})	2.642	2.590	2.538	2.418	2.353	2.307	2.414	2.349	2.262
Johnson - Gyrobifastigium (J26; D_{2d})	17.290	17.421	17.336	17.056	16.193	16.241	16.571	16.442	16.343
Johnson - Elongated Triangular Bipyramid (J14; D_{3h})	30.457	30.448	29.994	30.005	28.767	28.555	29.746	28.667	29.180
Johnson - Biaugmented Trigonal Prism (J50; C_{2v})	3.195	3.094	2.956	3.044	2.414	2.426	2.897	2.941	2.849
Biaugmented Trigonal Prism (C_{2v})	2.189	2.132	2.069	2.043	1.131	1.120	1.909	2.005	1.806
Johnson - Snub Disphenoid (J84; D_{2d})	6.049	5.912	5.685	5.698	4.676	4.701	5.480	5.452	5.371
Triakis Tetrahedron (T_d)	9.570	9.749	10.170	9.442	11.198	11.135	9.784	9.734	9.733
Elongated Trigonal Bipyramid (D_{3h})	25.671	25.708	25.325	25.170	24.646	24.428	25.372	24.543	24.405

Table S4. Continuous Shapes Measures (CShM) values (*SHAPE 2.1*) for the six-coordinate ring M^{III} ions in **1** – **7**.

Shape	Hexagon (D_{6h})	Pentagonal Pyramid (C_{5v})	**Octahedron (O_h)**	Trigonal Prism (D_{3h})	Johnson Pentagonal Pyramid (J2; C_{5v})
1[1]					
Mn1	31.397	28.576	**1.197**	16.816	30.843
Mn2	30.884	27.957	**0.998**	16.421	31.024
Mn3	31.372	28.163	**1.054**	17.065	31.168
Mn4	31.620	28.760	**1.070**	16.917	31.086
2					
Mn	31.221	28.327	**0.986**	16.646	20.659
3					
Mn	32.060	28.484	**0.805**	15.822	31.168
4					
Ga	31.571	28.279	**0.578**	16.133	31.527
5					
Ga2	32.784	26.315	**0.589**	14.222	30.006
Ga4	32.294	25.338	**0.723**	12.561	29.140
Ga6	31.909	25.389	**0.722**	12.448	29.193
Ga8	32.575	26.452	**0.575**	14.344	30.154
6					
Ga1	32.404	26.308	**0.845**	13.411	30.215
Ga2	31.881	26.760	**0.677**	13.468	30.540
Ga4	31.847	26.354	**0.582**	13.304	30.208
7					
Ga2	31.744	28.445	**0.394**	15.928	31.980
Ga3	31.923	26.300	**0.658**	13.388	30.370
Ga4	32.557	25.477	**0.825**	12.494	28.983
Ga5	32.296	27.896	**0.375**	15.010	31.503
Ga7	31.039	27.327	**0.475**	14.351	30.105
Ga8	32.629	27.315	**0.473**	14.167	30.879

Table S5. Continuous Shapes Measures (CShM) values (*SHAPE 2.1*) for the five-coordinate ring Ga^{III} ions in **5**, **6**, and **7**.

Shape	Pentagon (D_{5h})	Vacant Octahedron (C_{4v})	Trigonal Bipyramidal (D_{3h})	**Spherical Square Pyramidal (C_{4v})**	Johnson Trigonal Bipyramidal (J12; D_{3h})
5					
Ga1	31.354	1.363	5.500	**0.292**	7.851
Ga3	30.926	1.059	5.179	**0.326**	7.846
Ga5	30.929	0.999	5.134	**0.374**	7.852
Ga7	31.761	1.416	5.377	**0.184**	8.104
6					
Ga3	30.942	1.462	5.471	**0.218**	8.071
7					
Ga1	31.651	1.523	4.736	**0.226**	7.965
Ga6	30.965	1.571	5.538	**0.208**	8.153

Table S6. Continuous Shape Measurement (CShM) values (*SHAPE 2.1*) for the eight-coordinate central Na^+ ions of **1** and **2**.

Shape	**1**[1]	**2**
Octagon (D_{8h})	31.860	31.739
Heptagonal Pyramid (C_{7v})	25.349	26.446
Hexagonal Bipyramid (D_{6h})	13.327	13.411
Cube (O_h)	5.593	5.479
Square Antiprism (D_{4d})	3.420	4.081
Triangular Dodecahedron (D_{2d})	3.756	4.391
Johnson - Gyrobifastigium (J26; D_{2d})	16.680	17.110
Johnson - Elongated Triangular Bipyramid (J14; D_{3h})	28.537	29.026
Johnson - Biaugmented Trigonal Prism (J50; C_{2v})	5.035	5.541
Biaugmented Trigonal Prism (C_{2v})	**3.306**	**3.760**
Johnson - Snub Disphenoid (J84; D_{2d})	7.713	8.523
Triakis Tetrahedron (T_d)	6.420	6.380
Elongated Trigonal Bipyramid (D_{3h})	25.212	25.632

Table S7. Continuous Shape Measurement (CShM) values (*SHAPE 2.1*) for the nine-coordinate central Na^+ ions of **4**.

Shape	**4**
Enneagon (D_{9h})	36.140
Octagonal Pyramid (C_{8v})	25.378
Heptagonal Bipyramid (D_{7h})	17.948
Johnson Triangular Cupola (J3; C_{3v})	16.829
Capped Cube (J8; C_{4v})	5.853
Spherical-Relaxed Capped Cube (C_{4v})	4.128
Capped Square Antiprism (J10; C_{4v})	3.671
Spherical Capped Square Antiprism (C_{4v})	**2.309**
Tricapped Trigonal Prism (J51; D_{3h})	4.777
Spherical Tricapped Trigonal Prism (D_{3h})	3.572
Tridiminished Icosahedron (J63; C_{3v})	13.837
Hula-Hoop (C_{2v})	9.532
Muffin (C_s)	2.852

Table S8. Continuous Shape Measurement (CShM) values (*SHAPE 2.1*) for the four-coordinate peripheral Na^+ ions of **3**.

Shape	**Square Planar (D_{4h})**	Tetrahedron (T_d)	Seesaw (C_{2v})	Vacant Trigonal Bipyramid (C_{3v})
3				
Na	**2.230**	22.903	10.215	23.254

Table S9. Continuous Shapes Measures (CShM) values (*SHAPE 2.1*) for the six-coordinate peripheral Ga^{III} ion of **7**.

Shape	Hexagon (D_{6h})	Pentagonal Pyramid (C_{5v})	**Octahedron (O_h)**	Trigonal Prism (D_{3h})	Johnson Pentagonal Pyramid (J2; C_{5v})
Ga1L	30.012	26.434	**0.519**	14.175	29.929

Table S10. Structural feature comparison of **1** – **7**.

	1	**2**	**3**	**4**	**5**		**6**	**7**	
MC Composition									
Central Metal[a]	Dy^{III}	Dy^{III}	Dy^{III}	Yb^{III}	$Dy^{III}1$	$Dy^{III}2$	Y^{III}	$Ho^{III}1$	$Ho^{III}2$
Ring Metal	Mn^{III}	Mn^{III}	Mn^{III}	Ga^{III}	Ga^{III}	Ga^{III}	Ga^{III}	Ga^{III}	
Countercation	Na^{+} in central cavity	Na^{+} in central cavity	Na^{+} on periphery	Na^{+} in central cavity	Hpy^{+} in lattice		Hpy^{+} in lattice	Ga^{III} on periphery	
Bridging Dicarboxylate	iph^{2-}	tma^{2-}	$dnic^{2-}$	tma^{2-}	$dtba^{2-}$		$dnic^{2-}$	$dnic^{2-}$	
Measurement									
Avg. Adjacent Ring M^{III}-M^{III} Distance (Å)	4.59	4.60	4.59	4.64	4.65	4.65	4.67	4.66	4.66
Avg. Cross Cavity Ring M^{III}-M^{III} Distance (Å)	6.49	6.51	6.48	6.56	6.57	6.57	6.60	6.59	6.58
Ring $M^{III}_{Centroid}$-Ring $M^{III}_{Centroid}$ Distance (Å)	11.17	11.16	11.20	10.82	12.83		10.82	10.86	
Avg. Ln^{III}-Ring M^{III} Distance (Å)	3.81	3.81	3.77	3.74	3.73	3.73	3.71	3.72	3.73
Ln^{III}-M^{III}MP Distance (Å)	1.99	1.97	1.92	1.79	1.76	1.76	1.69	1.73	1.76
$O_{ox\ Centroid}$ - $O_{carbLn\ Centroid}$ Distance (Å)	2.70	2.67	2.61	2.55	2.54	2.55	2.62	2.58	2.59
Avg. Na-Ring M^{III} Distance (Å)	3.61	3.65	7.49	3.68					
Na-M^{III}MP Distance (Å)	1.58	1.66		1.65					
Na-O_{sol}MP Distance (Å)	0.71	0.60		0.49					
$O_{ox\ Centroid}$ - $O_{sol\ Centoid}$ Distance (Å)	2.67	2.67	2.65	2.52					
Avg. Ring M^{III}-$O_{carbM^{III}}$ Distance (Å)	2.13	2.13	2.16	1.97	1.93	1.92	1.98	2.00	1.99

Table S10 (continued). Structural feature comparison of **1** – **7**.

	1	**2**	**3**	**4**	**5**		**6**	**7**	
MC Composition									
Central Metal[a]	Dy^{III}	Dy^{III}	Dy^{III}	Yb^{III}	$Dy^{III}1$	$Dy^{III}2$	Y^{III}	$Ho^{III}1$	$Ho^{III}2$
Ring Metal	Mn^{III}	Mn^{III}	Mn^{III}	Ga^{III}	Ga^{III}	Ga^{III}	Ga^{III}	Ga^{III}	
Countercation	Na^+ in central cavity	Na^+ in central cavity	Na^+ on periphery	Na^+ in central cavity	Hpy^+ in lattice		Hpy^+ in lattice	Ga^{III} on periphery	
Bridging Dicarboxylate	iph^{2-}	tma^{2-}	$dnic^{2-}$	tma^{2-}	$dtba^{2-}$		$dnic^{2-}$	$dnic^{2-}$	
Measurement									
Ring $M^{III}_{Centroid}$ - $O_{carbM^{III}\ Centroid}$ Distance (Å)	2.03	2.03	2.06	1.87	1.82	1.82	1.90	1.90	1.89
Avg. Ring M^{III}-O_{sol}/N_{sol} Distance (Å)	2.47	2.44	2.33	2.30	2.22	2.21	2.25	2.18	2.15
Ring $M^{III}_{Centroid}$ - $O_{sol\ Centroid}$ Distance (Å)	2.29	2.26	2.19	2.14					
$O_{carbM^{III}\ Centroid}$ - $O_{sol\ Centroid}$ Distance (Å)	4.32	4.29	4.25	4.01					
Avg. O_{sol}/N_{sol}-Ring M^{III}-Ln^{III} Angle (°)	99.49	99.91	101.80	97.27	108.05	108.11	108.40	105.36	102.92
Avg. Ring M^{III}-O_{ox}-Ln^{III} Angle (°)	120.85	121.41	122.51	121.94	120.92	120.44	120.50	121.38	121.73

[a]For compounds **1**-**4** and **6**, the lanthanide ions are related by an inversion center; thus, there is only one unique lanthanide per dimer. For **5** and **7**, the lanthanide ions are not related by any symmetry elements; thus, each lanthanide ion and the corresponding [12-$MC_{M(III)N(shi)}$-4] unit is independent from the other.

Abbreviations: O_{ox} – oxime oxygen atom of the MC ring, O_{sol} – oxygen atom from either a solvent water or DMF molecule, N_{sol} – nitrogen atom of a solvent pyridine molecule, O_{carbLn} – the carboxylate oxygen atom of the dicarboxylate anion that is bound to the central Ln^{III} ion, $O_{carbM^{III}}$ – the carboxylate oxygen atom of the dicarboxylate anion that is bound to the ring M^{III} ion, O_{axial}/N_{axial} – the oxygen or nitrogen atoms along the *z*-axis of the ring M^{III} ions, and MP – the mean plane for the four atoms specified.

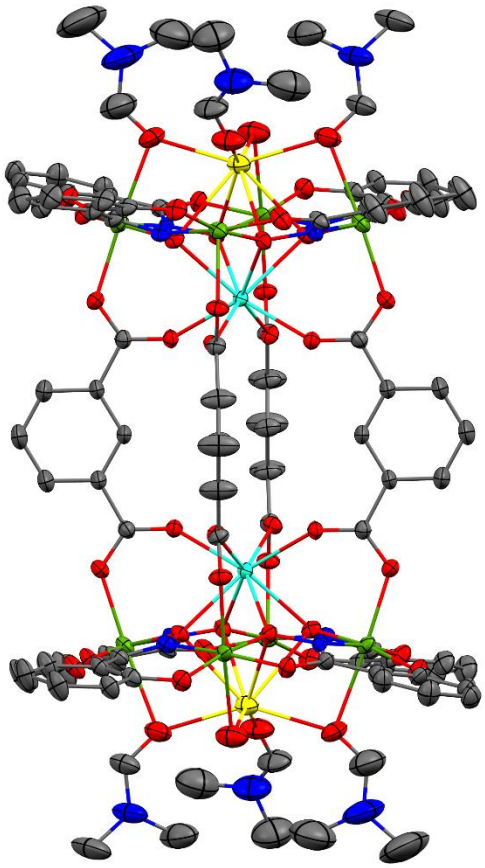

Figure S1. Single-crystal X-ray structure of DyNa[12-$MC_{Mn(III)N(shi)}$-4]}$_2$(iph)$_4$(H_2O)$_2$(DMF)$_6$•6H_2O•4DMF, **$Dy_2Mn_8Na_2$(iph)$_4$ (1)**.[1] The displacement ellipsoid plot is at the 50% probability level. Hydrogen atoms, lattice DMF and water molecules, and disorder have been omitted for clarity. Color scheme: light blue, dysprosium; green, manganese; yellow, sodium; red, oxygen; dark blue, nitrogen; and gray, carbon.

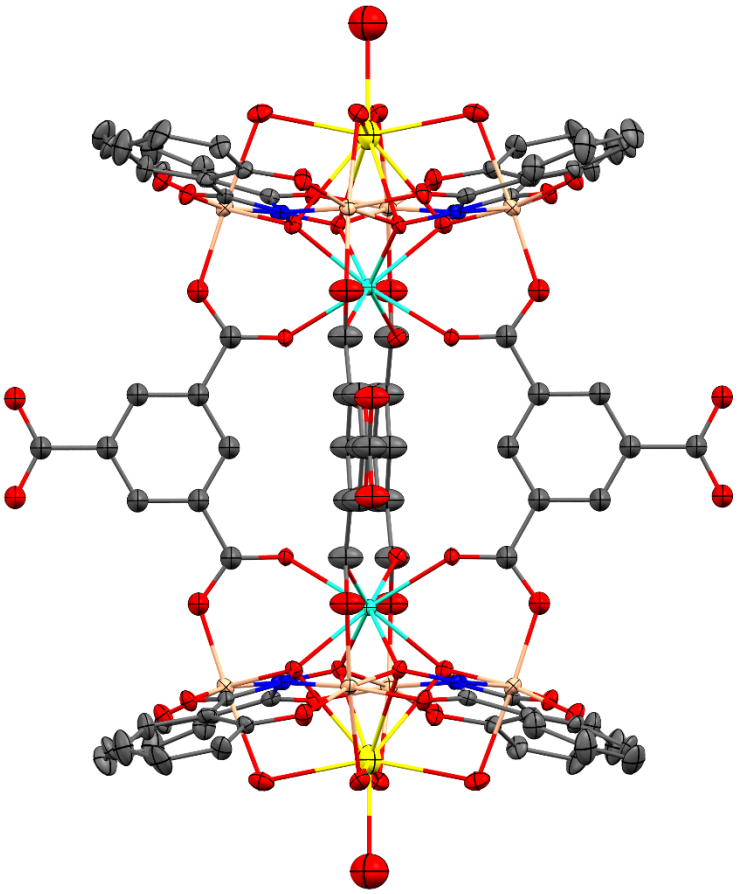

Figure S2. Single-crystal X-ray structure of $\{YbNa[12\text{-}MC_{Ga(III)N(shi)}\text{-}4]\}_2(tma)_4(H_2O)_{10}\bullet 3H_2O\bullet 15DMF$, $\mathbf{Yb_2Ga_8Na_2(tma)_4}$ (**4**). The displacement ellipsoid plot is at the 50% probability level. Hydrogen atoms, lattice DMF and water molecules, and disorder have been omitted for clarity. Color scheme: light blue, ytterbium; tan, gallium; yellow, sodium; red, oxygen; dark blue, nitrogen; and gray, carbon.

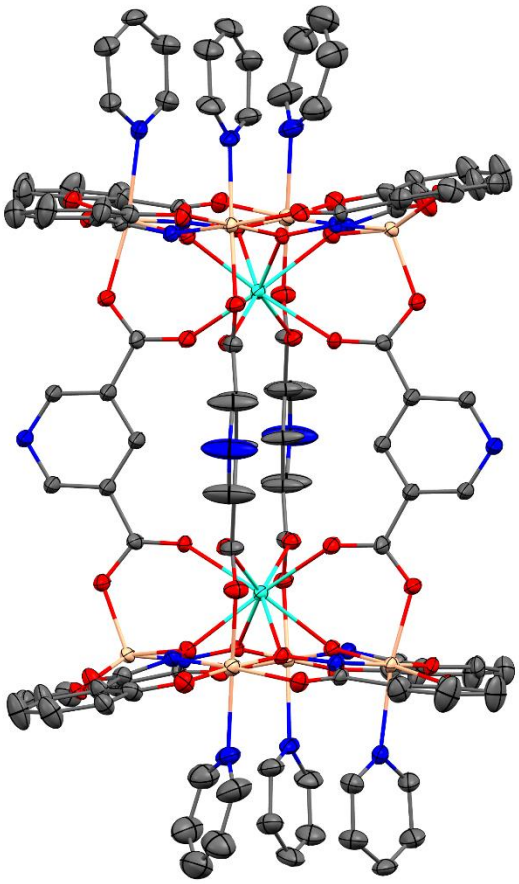

Figure S3. Single-crystal X-ray structure of $[Hpy]_2\{Y[12\text{-}MC_{Ga(III)N(shi)}\text{-}4]\}_2(dnic)_4(py)_6\bullet 4DMF$, $\mathbf{Y_2Ga_8(Hpy)_2(dnic)_4}$ (**6**). The displacement ellipsoid plot is at the 50% probability level. Hydrogen atoms, lattice DMF molecules, lattice pyridinium cations, and disorder have been omitted for clarity. Color scheme: light blue, yttrium; tan, gallium; yellow, sodium; red, oxygen; dark blue, nitrogen; and gray, carbon.

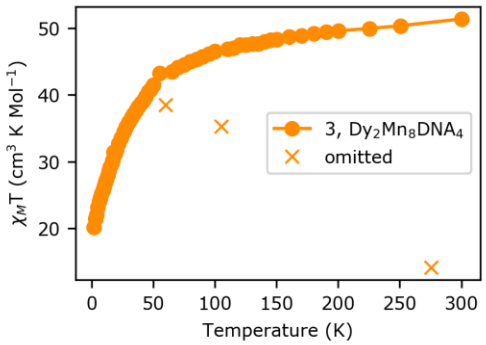

Figure S4. Powder magnetic susceptibility experiment for **3** from 2-300 K with an applied field of 2000 Oe (0.2 T). For clarity of presentation, the three points marked were removed from presentation in the main text. In each case these points are presumed erroneous, as the removed points deviate by >10% from their two nearest neighbors.

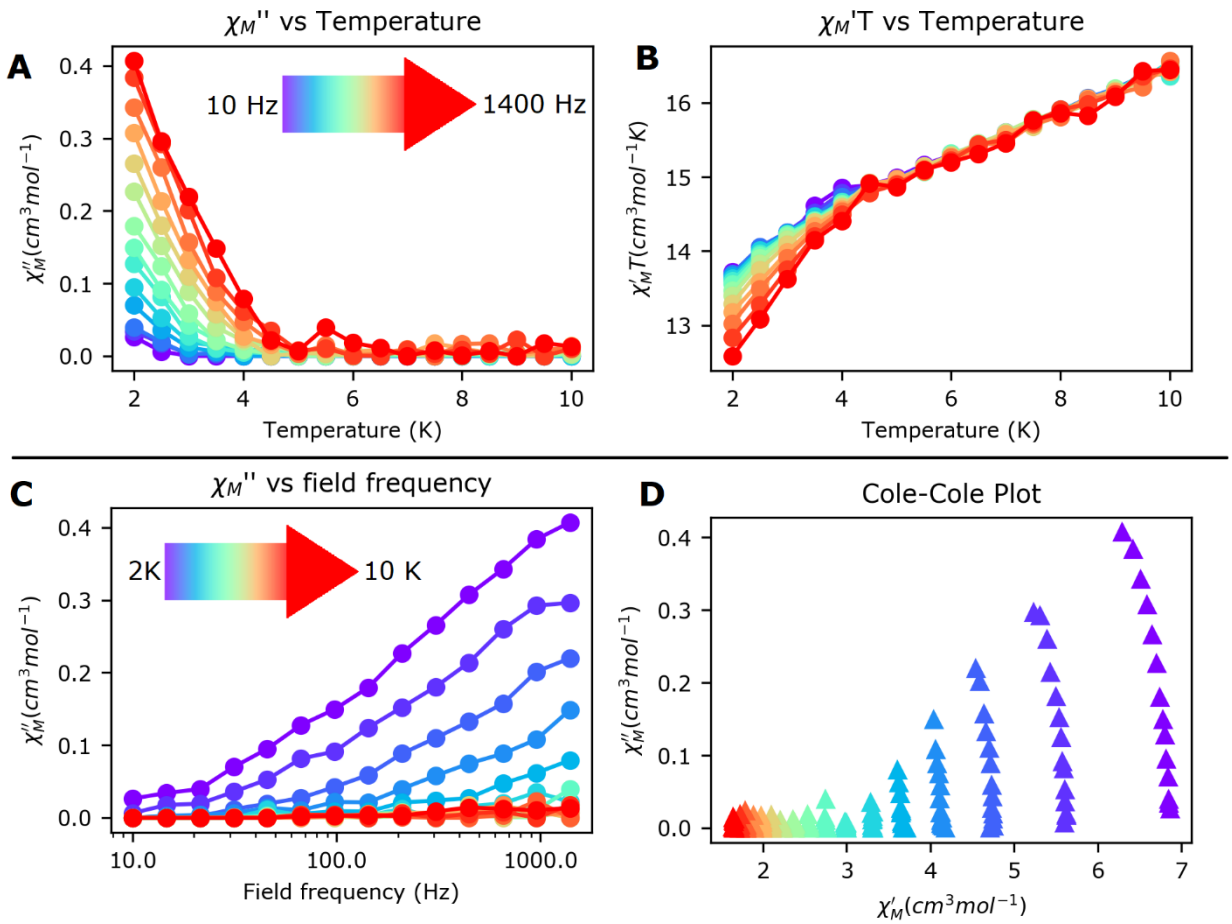

Figure S5. AC Susceptibility experimental results for complex **1**. Panels A&B share a common figure legend where the color gradient represents progression from 10-1400 Hz in 16 evenly spaced log-scale steps; panels C&D share a common figure legend where the color gradient depicts progression from 2-10 K in 0.5 K steps. All measurements performed with a 3 Oe drive field without a DC bias field. (A) Out-of-phase molar AC susceptibility (χ_M'') versus temperature for different drive field frequencies. (B) In-phase molar AC susceptibility (χ_M') versus temperature for different drive field frequencies. (C) χ_M'' versus drive-field frequency for different temperatures. (D) Cole-Cole plot depicting χ_M'' vs χ_M' for different temperatures.

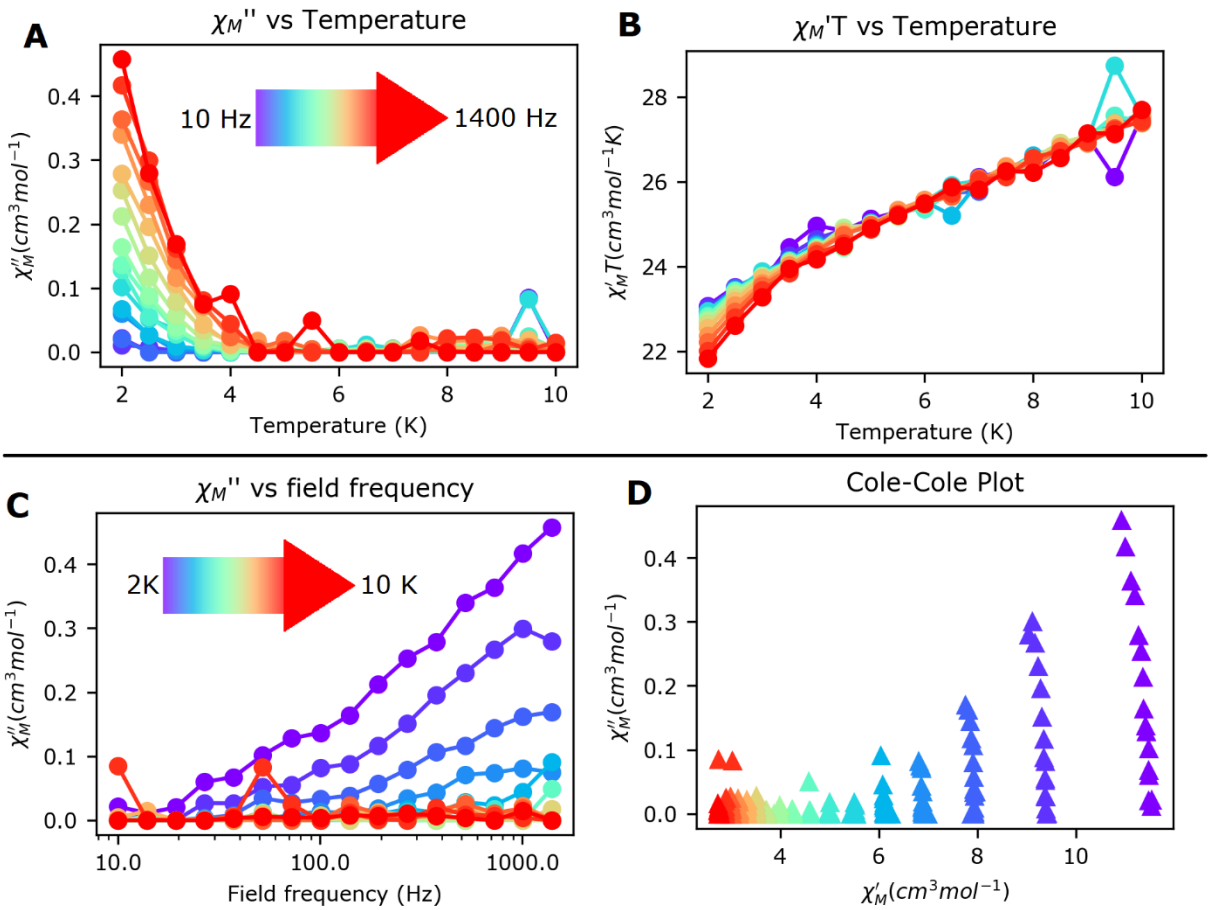

Figure S6. AC Susceptibility experimental results for complex **2**. Panels A&B share a common figure legend where the color gradient represents progression from 10-1400 Hz in 16 evenly spaced log-scale steps; panels C&D share a common figure legend where the color gradient depicts progression from 2-10 K in 0.5 K steps. All measurements performed with a 3 Oe drive field without a DC bias field. (A) Out-of-phase molar AC susceptibility (χ_M'') versus temperature for different drive field frequencies. (B) In-phase molar AC susceptibility (χ_M') versus temperature for different drive field frequencies. (C) χ_M'' versus drive-field frequency for different temperatures. (D) Cole-Cole plot depicting χ_M'' vs χ_M' for different temperatures.

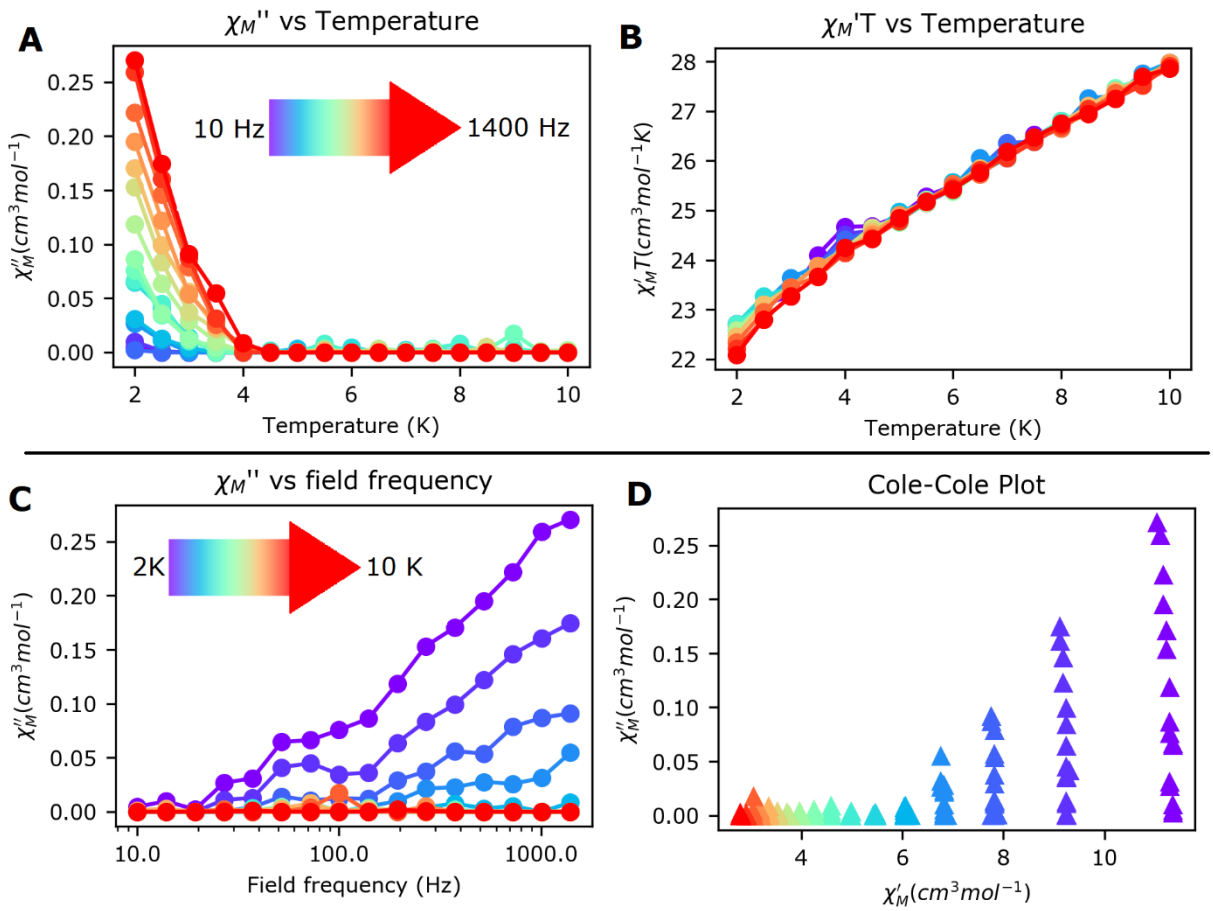

Figure S7. AC Susceptibility experimental results for complex **3**. Panels A&B share a common figure legend where the color gradient represents progression from 10-1400 Hz in 16 evenly spaced log-scale steps; panels C&D share a common figure legend where the color gradient depicts progression from 2-10 K in 0.5 K steps. All measurements performed with a 3 Oe drive field without a DC bias field. (A) Out-of-phase molar AC susceptibility (χ_M'') versus temperature for different drive field frequencies. (B) In-phase molar AC susceptibility (χ_M') versus temperature for different drive field frequencies. (C) χ_M'' versus drive-field frequency for different temperatures. (D) Cole-Cole plot depicting χ_M'' vs χ_M' for different temperatures.

References

1. Foley, C. M.; Armanious, M. A.; Smihosky, A. M.; Zeller, M; Zaleski, C. M. Syntheses and Crystal Structures of a Series of Manganese-Lanthanide-Sodium 12-Metallacrown-4 Dimers. *J. Chem. Crystallogr.* **2021**, *51*, 465 – 482. https://doi.org/10.1007/s10870-020-00870-1.